Cretaceous Research 112 (2020) 104425

Contents lists available at ScienceDirect

Cretaceous Research

journal homepage: www.elsevier.com/locate/CretRes

Cranial palaeopathologies in a Late Cretaceous mosasaur from the Netherlands

Dylan Bastiaans [a, b, c, d, *], Jeroen J.F. Kroll [e], Dirk Cornelissen [b], John W.M. Jagt [b], Anne S. Schulp [b, c, d]

[a] Universität Zürich, Paläontologisches Institut und Museum, Karl-Schmid-Strasse 4, 8006 Zürich, Switzerland
[b] Natuurhistorisch Museum Maastricht, De Bosquetplein 6-7, 6211 KJ Maastricht, the Netherlands
[c] Naturalis Biodiversity Center, Darwingweg 2, 2333 CR Leiden, the Netherlands
[d] Faculty of Geosciences, Utrecht University, Princetonlaan 8a, 3584 CB Utrecht, the Netherlands
[e] MUMC+, Department of Radiology, P. Debyelaan 25, 6229 HX Maastricht, the Netherlands

ARTICLE INFO

Article history:
Received 25 September 2019
Received in revised form
14 January 2020
Accepted in revised form 12 February 2020
Available online 28 February 2020

Keywords:
Trauma
Palaeopathology
Mosasaurs
Osteomyelitis
Maastrichtian
Intraspecific agonistic behaviour

ABSTRACT

Here we describe multiple pathological skeletal elements in a specimen assigned to a globidensine mosasaur as *Prognathodon* cf. *sectorius*. This individual, NHMM 2012 072, was recovered from the upper Lixhe 3 Member (Gulpen Formation, upper Maastrichtian) near Maastricht, the Netherlands. In all likelihood, it was bitten in the snout by a large, possibly conspecific mosasaur – and survived this attack. The specimen described here is among the very few with clear and unambiguous evidence of (very likely intraspecific) agonistic interactions amongst mosasaurs. Despite significant injuries, including partial amputation of the premaxilla, this animal initially recuperated from the encounter, but the subsequent infectious processes as a result of this attack were still ongoing at the time of death. Radiological and morphological features suggest chronic osteomyelitis which led to loss of bone within the left maxilla, which probably hampered the ability to feed, potentially contributing to its demise. This case study illustrates the potential of integrative three-dimensional approaches in palaeopathological studies to provide a much more comprehensive and detailed description of alterations and underlying physiological processes.

1. Introduction

On rare occasions, diseases and injuries sustained during the lifetime of an organism can be preserved in the fossil record, in the form of osseous lesions and exostoses (Moodie, 1917, 1923; Rothschild and Martin, 2006). Palaeopathology, or the study of these records of disease and trauma in archaeology and palaeontology, may provide a better insight into disease acquisition, soft tissue anatomy, healing strategies and even behavioural aspects of extant and extinct taxa (Moodie, 1917, 1923; Monastersky, 1989, 1990; Rothschild and Martin, 2006; Reisz et al., 2011; Anné et al., 2015). Although many palaeopathological surveys have been undertaken in dinosaurs and archosaurs in general, the majority of squamates have remained largely understudied (e.g., Monastersky, 1990; Bell, 2010; Bell and Currie, 2010; Rothschild, 2013; Foth et al., 2015; Anné et al., 2015; Hedrick et al., 2016; Xing et al., 2018). However, research on pathologies in mosasaurs (extinct Late Cretaceous marine squamates; Russell, 1967) took off early, as is demonstrated in papers by Mudge (1877), Dollo (1882) and Gaudry (1890). Their (mostly descriptive) works were succeeded by numerous reports on both traumatic (e.g. Meijer, 1985; Mulder, 1985; Bell and Martin, 1995; Martin and Bell, 1995; Lingham-Soliar, 1998, 2004; Everhart, 2008) and non-traumatic conditions (e.g. Rothschild and Martin, 1987, 1993, 2006; Martin and Rothschild, 1989; Monastersky, 1990; Rothschild and Tanke, 1992; Mulder, 2001; Schulp et al., 2004), prompting the first hypotheses on their underlying behavioural implications.

Multiple pathological specimens of various mosasaur genera have been recovered from the Maastrichtian type area (southeast Netherlands, northeast Belgium); these provide a glimpse into the interactions and trophic relationships of these marine squamates that inhabited this latest Cretaceous ecosystem (e.g. Kruytzer, 1957; Mulder, 1985, 1999, 2001; Lingham-Soliar, 1998, 2004; Schulp et al.,

* Corresponding author. Universität Zürich, Paläontologisches Institut und Museum, Karl-Schmid-Strasse 4, 8006 Zürich, Switzerland.
E-mail address: dylan.bastiaans@pim.uzh.ch (D. Bastiaans).

https://doi.org/10.1016/j.cretres.2020.104425

2004, 2006). This record has subsequently been augmented by new finds from other locations (e.g. Bell and Barnes, 2007; Everhart, 2008, 2012; Einarsson et al., 2010). Many pathological studies rely on external morphological comparisons only, despite the availability of histological, isotopic, other geochemical and radiological techniques (Straight et al., 2009; Peterson and Vittore, 2012; Anné et al., 2015; Hedrick et al., 2016). In the present contribution we report on a palaeopathological case study of a recently discovered specimen of mosasaur, assigned to *Prognathodon* cf. *sectorius* (NHMM 2012 072) from the type area and illustrate opportunities that are provided by modern day integrative approaches (e.g. CT and 3D-visualizations). Inherently destructive palaeohistological approaches were not applied, because this particular specimen represents a unique occurrence of a rare taxon.

2. Materials and methods

2.1. Institutional abbreviation

NHMM: Natuurhistorisch Museum Maastricht, Maastricht, the Netherlands.

2.2. Material

The specimen described here, NHMM 2012 072 was discovered on September 17, 2012 by quarry operator Carlo Brauer. It originates from the upper third of the flint-rich Lixhe 3 Member of the Gulpen Formation (c. 68,3 Ma; Keutgen, 2018) of the former ENCI HeidelbergCement Group quarry, located south of Maastricht (Fig. 1), making it the oldest known identifiable skeletal mosasaur occurrence from the Maastrichtian type locality known to date (Jagt and Jagt-Yazykova, 2012; Schulp and Jagt, 2013; Keutgen, 2018). Bone material from these lower strata is preserved in a fashion that differs markedly from that of vertebrates found higher up in section. A major difference is the presence and subsequent oxidation of pyrite and marcasite in the matrix and the fossil bone producing sulphur oxides, which in turn react with the carbonates of the matrix, resulting in a thin gypsum veneer on the surface of the fossil (Ritsema and Groenenberg, 1993). This gives the fossil a progressively greyish appearance with time, and will require additional curatorial attention in order to prevent chemical disintegration of the bones.

The disarticulated assemblage includes partial sections of the maxillae, dentaries, braincase and parietal (Fig. 2), as well as various elements of the axial skeleton. Some bone surfaces are heavily abraded, which is markedly different from what is generally encountered higher up in the section. The presence of shed teeth of odontaspidid sharks, together with tooth marks on the right dentary surrounding the neural foramen between the fourth and fifth tooth positions, suggest at least some degree of scavenging by pointed-toothed organisms.

Although preparation is still ongoing, some inferences can be made based on the available skeletal material. Tooth morphology, including a swollen tooth base, labiolingually flattened crowns and sharp carinae, suggest affinities with *Prognathodon sectorius* (Schulp and Jagt, 2013). Extrapolation of the alveolar spacing in a jaw section yielded an estimated body length of around thirteen metres. Together with the fused haemal arches, this enormous length would suggest the ontogenetic age to be close to maximum attainable size (i.e. full maturity).

2.3. Terminology

The terminology used here to describe the appearance and underlying disease processes, as well as the manner of description and classification of the various pathologies (e.g. traumatic, infectious, traumatic-infectious, developmental and idiopathic) and their respective criteria, follow the guidelines as presented by Hanna (2002) and Foth et al. (2015).

2.4. CT Scanning

The dentaries were CT scanned using a Philips Brilliance Big Bore at the Universitair Medisch Centrum (UMC) Utrecht, the Netherlands, at 1-mm slice thickness, 120 kV, tube current of 263 mA, and an exposure time of 4031 ms, rendering 363 axial slices in 512 × 512 pixels. Elements from the upper jaw were CT scanned using a Siemens Somatom Definition Flash scanner at the Maastricht University Medical Center (MUMC+), Maastricht, the Netherlands, at 600-μm slice thickness, 230 kV, tube current of 600 mA, and an exposure time of 500 ms, rendering 465 axial slices in 512 × 512 pixels. The resulting DICOM stacks were converted to 3D models using a combination of Avizo v. 8.1, Meshlab v.1.3.2 and Polyworks workspace manager v12.1.23 at the Rheinische Friedrich-Wilhelms-Universität Bonn, Germany and Mimics v21.0 at the Paläontologisches Institut und Museum Zürich, Switzerland. The specimen of the Asian water monitor (*Varanus salvator*, PIMUZ A/III 1493), originally from the Zoo Zürich, was euthanised after contracting pododermatitis on the 14th of May 1981. It was subsequently macerated by Dr. Rieppel and taxidermist Schoch and assembled by Badertscher & W. Etter in 1981. The monitor currently part of the palaeontological teaching collection of the Paläontologisches Institut und Museum (Zürich, Switserland) was CT scanned using a Nikon XT H 225 ST at the Irchel (central) campus of the University of Zürich (Switzerland), at 300-μm slice thickness, 195 kV, tube current of 36 mA, rendering 771 slices in 1314 × 2492 pixels with an isotropic voxel size of 77,643-μm. The resulting tiff stacks were converted to 3D models using Mimics Materialise Innovation Suite v. 21.0 at the Paläontologisches Institut und Museum (PIMUZ), Universität Zürich (Zürich, Switzerland).

3. Description

In the following section the pathological features of NHMM 2012 072 will be discussed on the basis of their unique morphology in comparison to normal healthy bone.

3.1. External morphology - premaxilla

The anteriormost section of the premaxilla exhibits a rugose surface texture that extends dorsomedially from the tooth bases. Anterioventrally within this rugose-textured surface is a subcircular depression of roughly two centimetres in diameter (a in Fig. 3B). The rugose area is bordered dorsally by a small, yet distinct ridge of smooth cortical bone extending laterally from the anteriormost neurovascular canal of the premaxillary (b in Fig. 3A, B). Projecting dorsally from the second and sole remaining left premaxillary tooth present, a small pea-like bony structure is visible (c in Fig. 3A, B). An elongated lesion is seen on the left side of the anteriormost premaxillary neurovascular foramen, interconnected with the foramen ventrally and separated merely by a bridge of smooth bone dorsally (d in Fig. 3A).

Situated predominantly posteriorly on the right side of the premaxilla and right maxilla, a roughening of the bone surface can be distinguished (e in Fig. 3A). Very little smooth cortical bone can be differentiated in this area, in comparison to other abnormal regions.

The premaxilla shows an elongate, healed lesion that is oriented anteroposteriorly, starting near the left premaxillary-maxillary suture, slightly to the left of the anteroposterior central line (f in

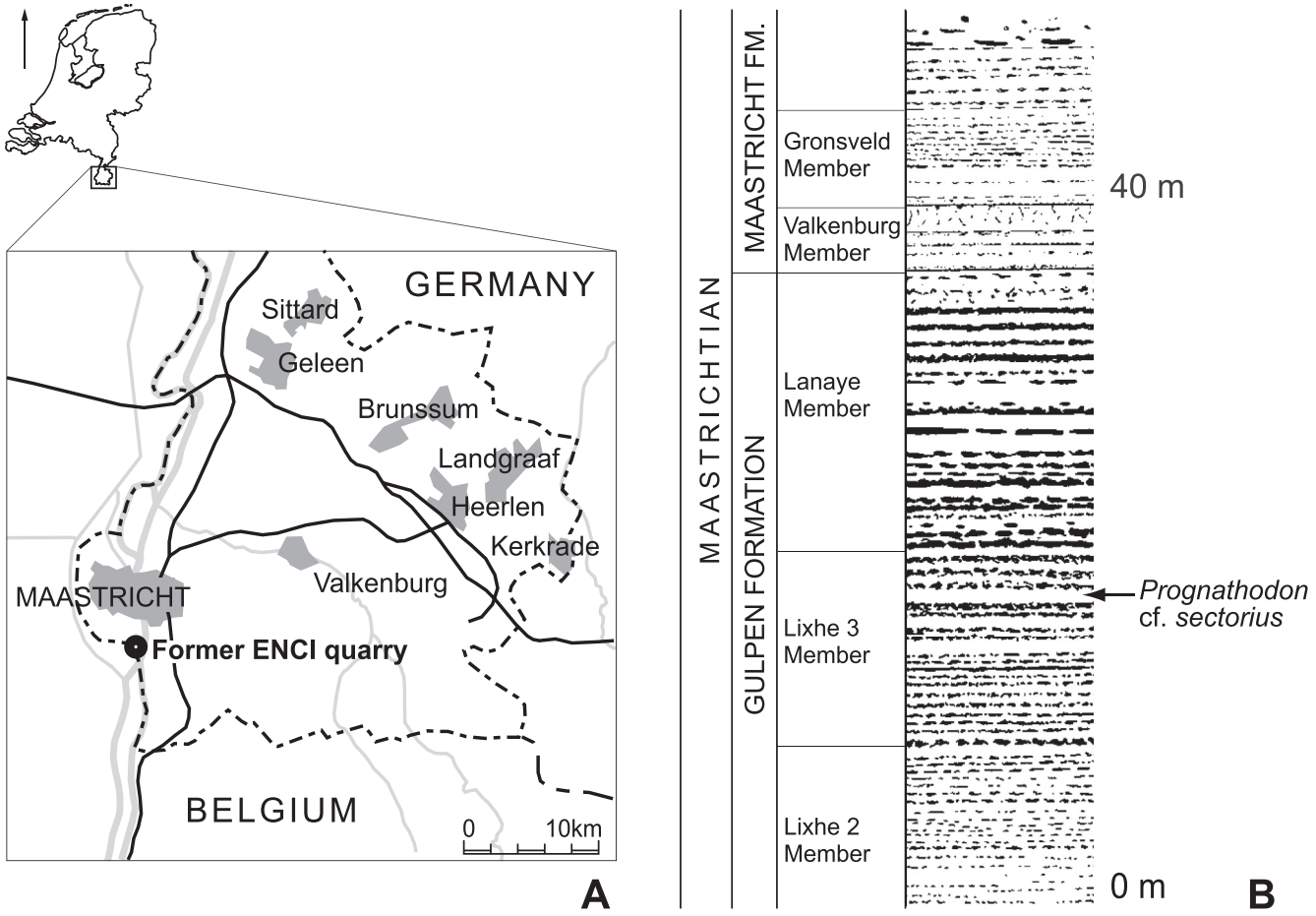

Fig. 1. Provenance area (**A**) and stratigraphic position (**B**) of *Prognathodon* cf. *sectorius* NHMM 2012 072.

Fig. 3A, B). Although posteriorly similar in appearance to the right lateral premaxillary surface, i.e., with a rugose appearance, the anteriormost section of the elongated bony protrusion consists of a smooth bone surface, only intermittently interrupted by tiny pits. Along the lateral edge of the lesion a broadened section is bordered by the left premaxilla-maxilla suture, displaying a heavily distorted surface texture with various depressions and of a distinctly pitted nature. Laterally, three distinct oblong pits (g in Fig. 3A, B) on the left maxilla, along with local depressions in the surface layer and numerous smaller pits, closely match those of the adjacent premaxilla in both extent and appearance.

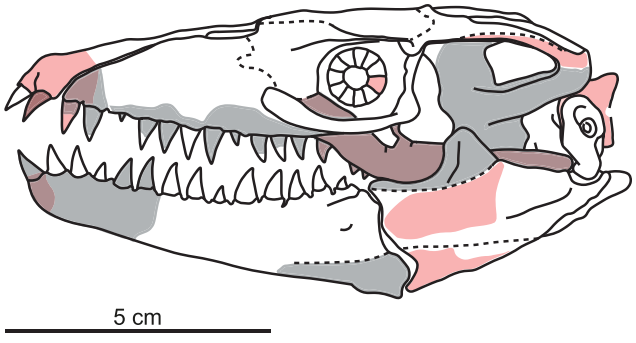

Fig. 2. Skull elements of *Prognathodon* cf. *sectorius* (NHMM 2012 072) preserved shown in red for the left side and in grey for the right side. Skull outline adapted from Dortangs et al. (2002). (For interpretation of the references to colour in this figure legend, the reader is referred to the Web version of this article.)

3.2. External morphology - maxilla

Some evidence of reactive bone can also be distinguished near the base of the first maxillary tooth on the left side which is situated ventrolaterally from the anteriormost oblong pit (h in Fig. 3B), enclosed by depressions anteriorly and posteriorly. The swollen appearance of the tooth base differs from that of the less strongly swollen premaxillary tooth base. This might, in part, be due to a combination of taphonomic overprinting (i.e. deformation) and the phylogenetically distinct appearance of the tooth base (i.e. 'prognathodont' condition). The exostosial bone near the left premaxilla-maxilla suture, together with evidence of necrosis and exostiosal bone growth on the tip of the premaxilla, possibly related to smaller gouges located more posteriorly, give the overall bone a distinct appearance that diverges notably from the natural state.

3.3. External morphology - dentary

A callus (i in Fig. 4C, D) is present on the anteriormost section of the left dentary. This callus is centrally located on the lateral side of the dentary fragment, directly beneath the first tooth position. A small depression is surrounded by a rugose area. In contrast to its counterpart, the preserved part of the left dentary completely lacks neural foramina in the anterolateral side, and shows the

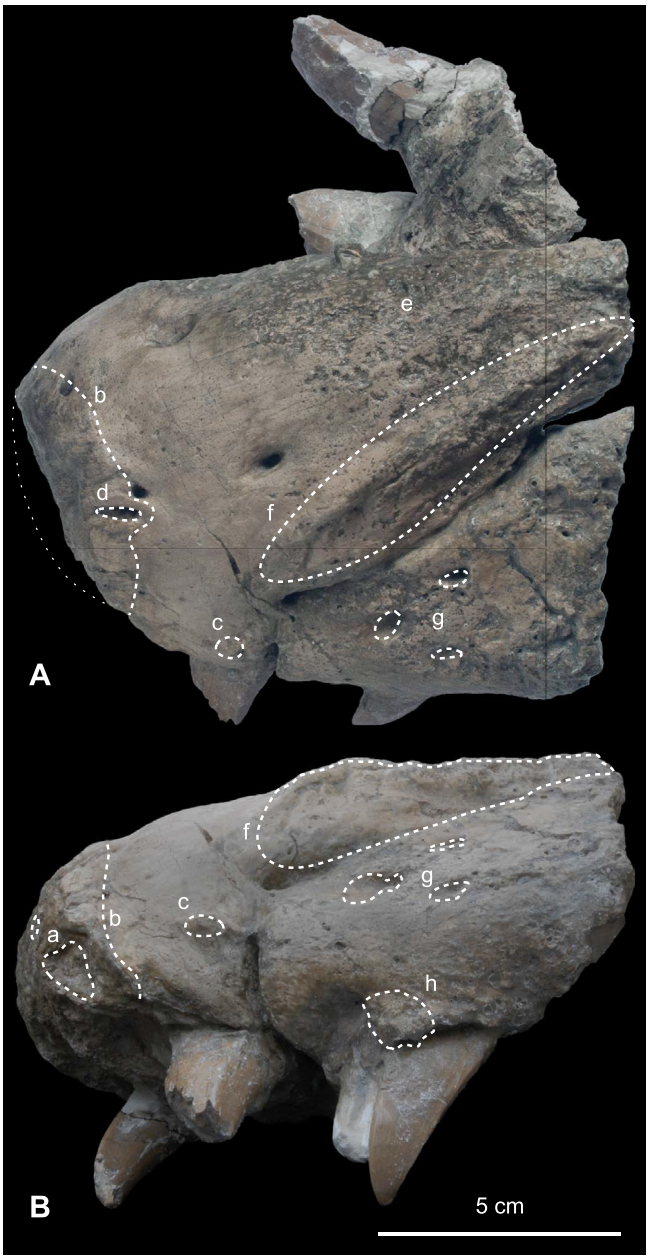

Fig. 3. *Prognathodon* cf. *sectorius* left maxilla and premaxilla of NHMM 2012 072 in (**A**) dorsal and (**B**) left lateral view. The letters denote the various abnormalities visible on the exterior of the elements of the upper jaw. Note the extensive damage to the anteriormost section of the premaxillary (a–d) and to the area on the left lateral side surrounding the premaxillary-maxillary suture (f–h). The rugosity on the right lateral side visible on the premaxillary (e) is most likely associated with *post-mortem* bacterial erosion.

enlargement of the ventrally located foramina. The right dentary displays a small lesion anterolateral to the anteriormost tooth position and directly adjacent to a large neurovascular foramen (j in Fig. 4A, B).

3.4. Overall radiological appearance

The rugose anteriormost section of the premaxillary is more radiolucent compared to the areas of normal density directly posteriorly (Fig. 5). The former region is characterised by a rugose surface area centred around a roughly 2-cm-wide depression (a in Fig. 3B) capped by a smooth dorsoventral growth extending laterally in both directions (b in Fig. 3A, B). This radiolucent region is markedly different from the region surrounding the two adjacent openings in the anteriormost premaxillary (d in Fig. 3A, and its neurovascular foramen), which shows bone of a normal radiological appearance.

This rugose area can be linked to the elongate lesion that extends from the elevated structure on its dorsal edge (d in Fig. 3A). However, the bony bridge in between these two adjacent holes in the anteriormost portion of the premaxilla is also visible, showing normal density. The small protrusion located near the sole surviving premaxillary tooth on the left lateral side, near the suture, has a density that is similar to the above-mentioned rugose structures (c in Fig. 3A, B).

The large rugose area (e in Fig. 3A), primarily positioned right laterally from the anteroposteriorly-oriented ridge on the premaxillary, is recognised by external to internal loss of bone, with little or no decrease in density from its natural state. This can further be discerned from infectious processes, as no signs of bone repair or reactive bone growth are observed. This homogeneous erosional pattern of bone surface in the affected area is even present on the antero-posteriorly-oriented reactive bony growth, as well as other skeletal elements including the medial surface of the lower jaw elements. As a result, this erosion-based rugosity might be attributable to *post-mortem* bacterial erosion.

The radiodensity of the ridge-like protrusion (f in Fig. 3A, B) and the left maxillary (g in Fig. 3A, B), is significantly lower in comparison to the surrounding regions, including the large aberrant region on the right lateral premaxillary. The most pronounced differences in density can be observed in the posterior two-thirds, mainly concentrated around halfway through the elongated anteroposterior exostosis of the premaxillary, and the adjacent section of the left maxillary. Furthermore, the bony architecture surrounding the first maxillary tooth base seems to have been altered as well, with emphasis on the small tubular radiolucencies extending towards the tooth base and the ventral surface of the maxillary.

3.5. Specific radiological appearance

The anterior premaxilla is more radiolucent when compared to the section directly posterior to the anterior premaxillary neurovascular foramen (Fig. 5B). In contrast, the external bone surface of most of the premaxillary, is covered by a layer of thick, compact bone of ten to twelve millimetres in thickness. The thickness of the same layer in the anteriormost and posterior section (i.e. at the base of the exostosial ridge) of the premaxillary is reduced to merely a couple of millimetres at most. This does not appear to be an artifact of preservation, as little *post-mortem* deformation or compaction has occurred at this end, and only minor erosion occurred. In transverse view, the ridge-like structure of the premaxillary shows a similar pattern (Fig. 5C). The reduced thickness of the outer highly dense (cortical) bone layer is restricted to the area underneath the ridge and the left maxillary, suggesting a correlation between the two. The cortical bone layer seems to have been unaffected on the right side of the premaxillary. A small triangular-shaped concentration of less dense irregular bony material can be distinguished underneath the ridge-like protrusion which can be traced along the entire length of this exostosis.

Although difficult to recognize, at the first premaxillary tooth position, faint contours of the alveoli on both sides are present in the radiographs. The alveolar cavity is largely unaffected at its natural margins, yet appears partially filled by new, highly vascularised tissue (Fig. 5A).

The most dramatic variations in radiolucency are visible near the oblong lesions of the maxillary and the depression lateral from the suture line on the premaxillary.

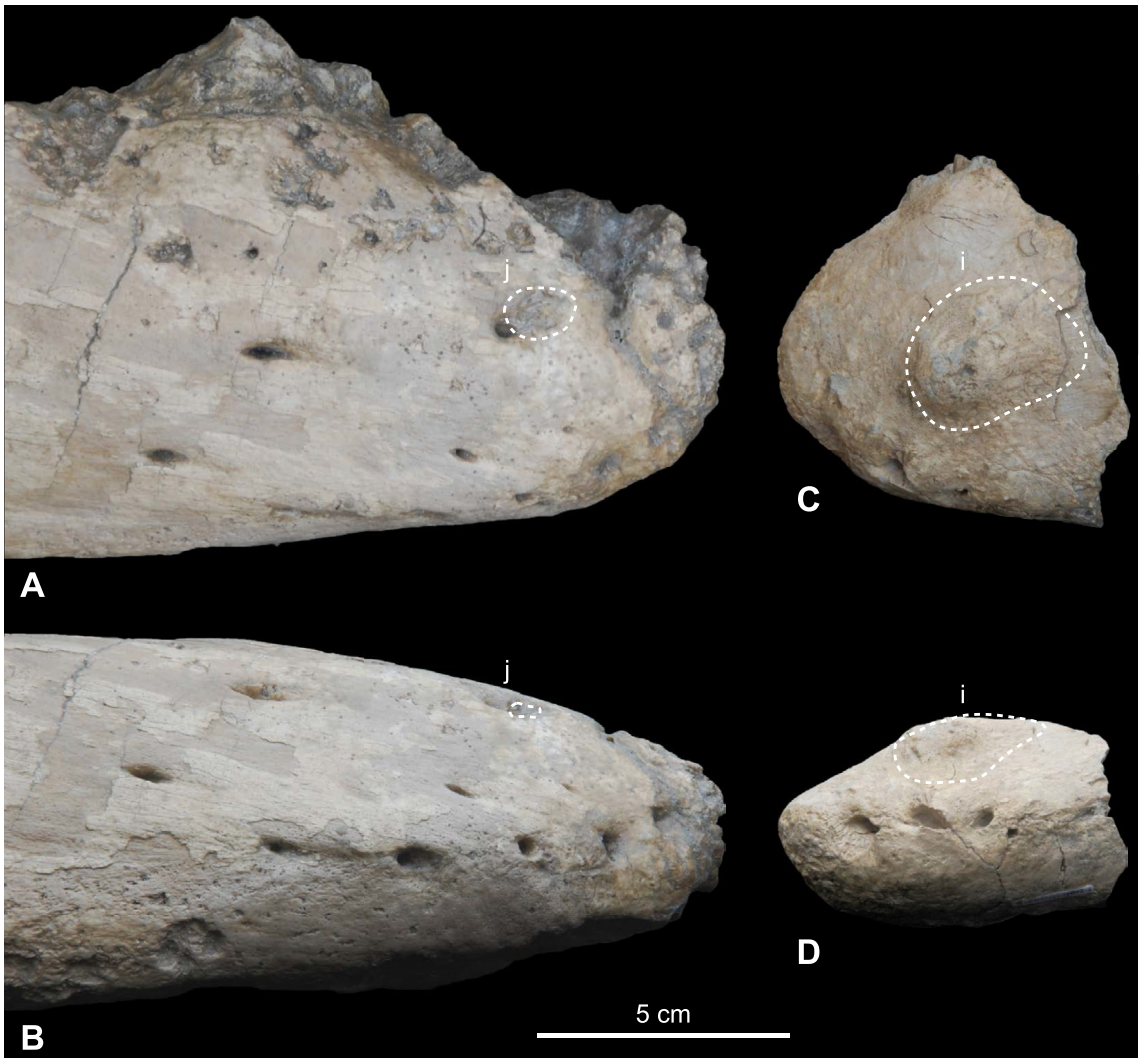

Fig. 4. *Prognathodon* cf. *sectorius* NHMM 2012 072 anterior dentary sections. (**A**) Right dentary in right lateral (**A**) and ventral (**B**) view; left dentary in left lateral (**C**) and (ventral (**D**) view, respectively. Notice the callus formation on the anteriormost section of the left dentary (i). When comparing the two dentary section, a striking difference is the complete lack of neural foramina on the surface of the left dentary fragment (**D**). Furthermore, slight widening of the neurovascular canals, visible in ventral view, can be observed. However, this could be due to preservation and preparation artifacts (**D**). A small, less conspicuous lesion can be identified in the anteriormost one-third of the right dentary fragment (j).

Particularly in the left maxilla, canals developed in the subsurface of this irregular and distinctly less dense bony material (Fig. 6). The extent, position and orientation of the patterns observed suggest a common origin for all or most radiolucent areas, as these all appear to be in comparable states of bone remodelling and display a comparable number of radiodensity changes.

Similar to the ridge-like exostosis on the premaxillary, which is bordered by bone of normal density on its right lateral side, the irregular surface concentrated around the oblong holes is also bordered by normal (dense) bone on its left lateral side. The area of reduced density that extends posteroventrally from the oblong holes on the maxillary, connects to the maxillary tooth base dorsolingually. The latter is indicated by an area of reduced density at this end of the tooth base in comparison to its anterior side.

The distribution of the canals underlying the pitted maxillary is best observed in coronal view (Fig. 6A). The lesions on the exterior of the bone are interconnected, forming a single central canal that runs anteroposteriorly throughout the maxillary (Fig. 6B, C). The internal bony architecture enclosing this large tubular maxillary network differs in appearance from the sharply defined structures visible in the neurovascular architecture of the premaxillary. Furthermore, the latter displays a highly organised interaction of the two dorsal pairs of canals and the pair of horizontal neurovascular tubular structures, while the former display different shapes, sizes and orientation between one another. It is therefore highly unlikely that the maxillary canals are part of a structured network of neurovascular tubules, as illustrated by the difference in canal morphology as mentioned above, and the presence of additional canals extending from the lateral subsurface of the maxillary.

The left dentary fragment has no obvious neural foramina on the (antero)lateral surface and large ventral foramina (Fig. 4). The radiological appearance (especially in coronal view) of the left dentary fragment, however, displays a normal neurovascular architecture with the anterioventrally projecting canals connecting to the foramina visible on the outer surface (Fig. 7). The regularly spaced neural branching pattern is similar to the condition in the opposite dentary, with dorsal offshoots connecting to the tooth margins and anterioventrally to the foraminal canals. The thickness and spacing of these canals is nearly identical in both dentary fragments, suggesting that the external damage visible concerning the widening of the foramina is most likely non pathological in nature (i.e. preparation or preservation artifacts).

The bony callus that extends from the lateral surface of the left dentary fragment, shows a distinct radiolucent cleft in transverse

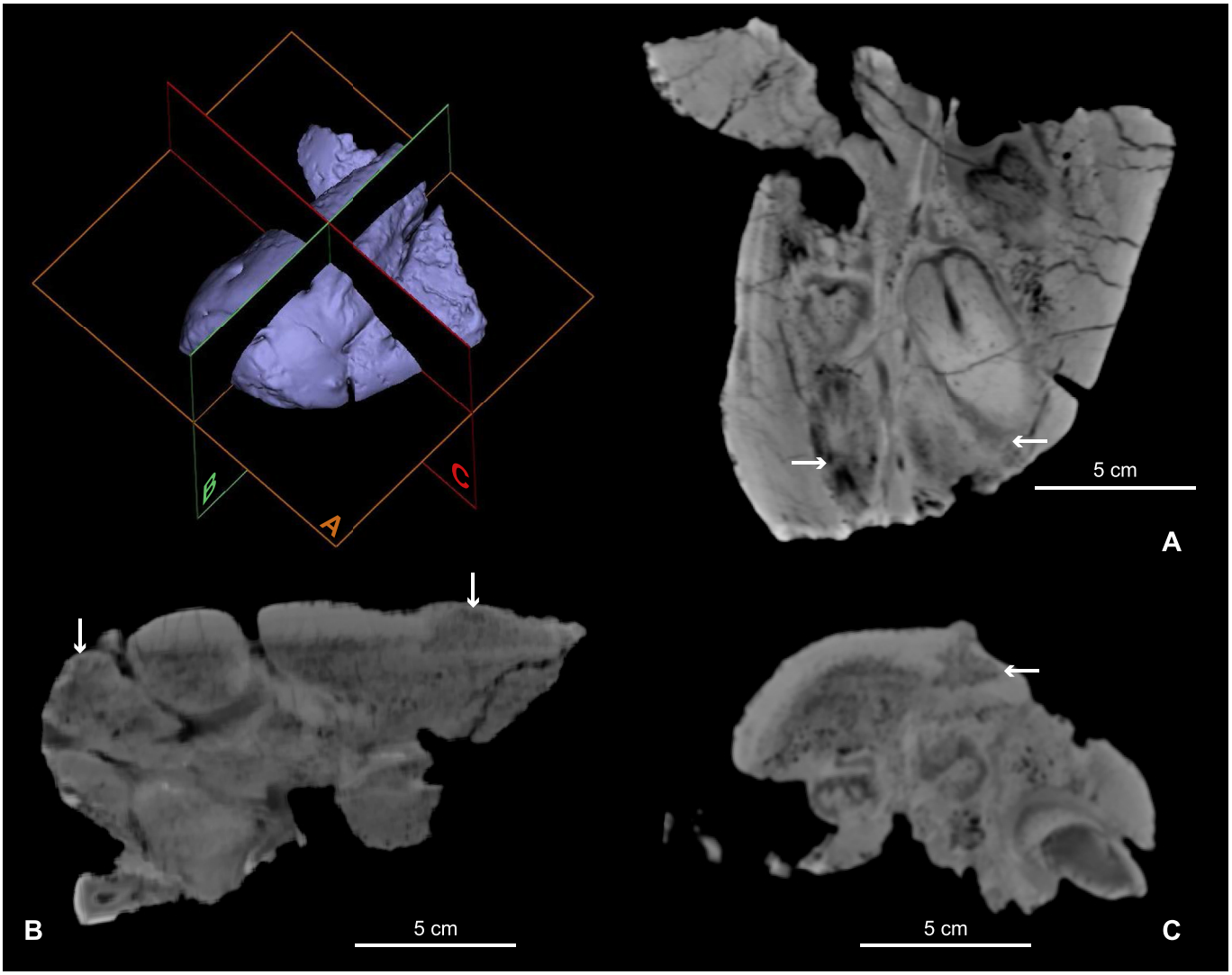

Fig. 5. *Prognathodon* cf. *sectorius* NHMM 2012 072 anterior segments of both maxillae. Clockwise from left to right: a 3D reconstruction using accompanied viewer software; (**A**) CT-slice in coronal view. Notice that the alveoli for the anteriormost premaxillary teeth are still present internally despite being absent externally (arrows); (**B**) CT-slice in sagittal view, showing the thickness of the outer bone layer (arrows), regularly interrupted by neurovascular channels; (**C**) CT-slice in axial view, illustrating the density changes underneath the ridge-like structure located anteroposteriorly along the premaxilla-maxilla suture (arrow). Notice that the bacterial erosion on the right lateral side of the premaxillary has not resulted in (significant) density differences. Furthermore, the severe decrease in the density is restricted to the left maxilla and adjacent section of the premaxilla and its anteriormost portion (**B**,**C**). The decreased density surrounding the right maxillary tooth can be explained by the presence of original limestone matrix.

view (Fig. 7A). The radiolucent cleft is centred in the bony exostosis, and extends nearly seven millimetres into the subsurface. The positioning of exostosial growth and its architecture suggests that the radiolucent cleft may in fact be related to the underlying cause of the damage to the dentary fragment. A second and much larger fracture with a wide spacing shows no sign of healing or reactive bone growth. The large amount of remodelling and reactive growth on the other fragments of the feeding apparatus, makes it more likely to be a consequence of post-depositional fracturing. The semicircular radiolucency visible in transverse view, representing the central neurovascular canal anteroposteriorly-oriented in the dentaries, is surrounded by non-reactive and regularly structured bony architecture.

3.6. 3D-modelling of pathologies

Three-dimensional visualisation of the dense external (cortical) bone layer (Fig. 8A, B), the infill of the triangular-shaped irregularity underneath the exostosial ridge on the premaxilla (Fig. 8C, D), and the infill of the canals underlying both the foramina of the premaxilla and the oblong holes of the left maxilla (Fig. 9), provides insight into the internal remodelling. The visualisation of the anomalous structure underlying the subsurface directly underneath the anteroposterior ridge-like exostosis, when compared to the adjacent normal cortical and subcortical bone layer, clearly shows the common origin of these abnormalities, as no abnormal irregular bony architecture was visible underneath the remainder of the premaxillary cortex.

The thickness of the cortical bone layer shows a distinct decrease from the right lateral side of the premaxillary to the left (Fig. 8A). The overall thickness of the cortical bone layer seems consistent on the right side of the premaxillary up to reaching the edge of the ridge-like structure, where it slightly thickens, before decreasing significantly on the left lateral side of the same structure, enclosed by another thickened section before reducing again significantly on the maxillary. This clearly shows that the focus of this pathological bone remodelling was centred around the left slope of the ridge-like growth, and the oblong holes in the maxillary. A virtual infill of the triangular anomaly that underlies the premaxillary ridge visualises the extent and shape of the reactive

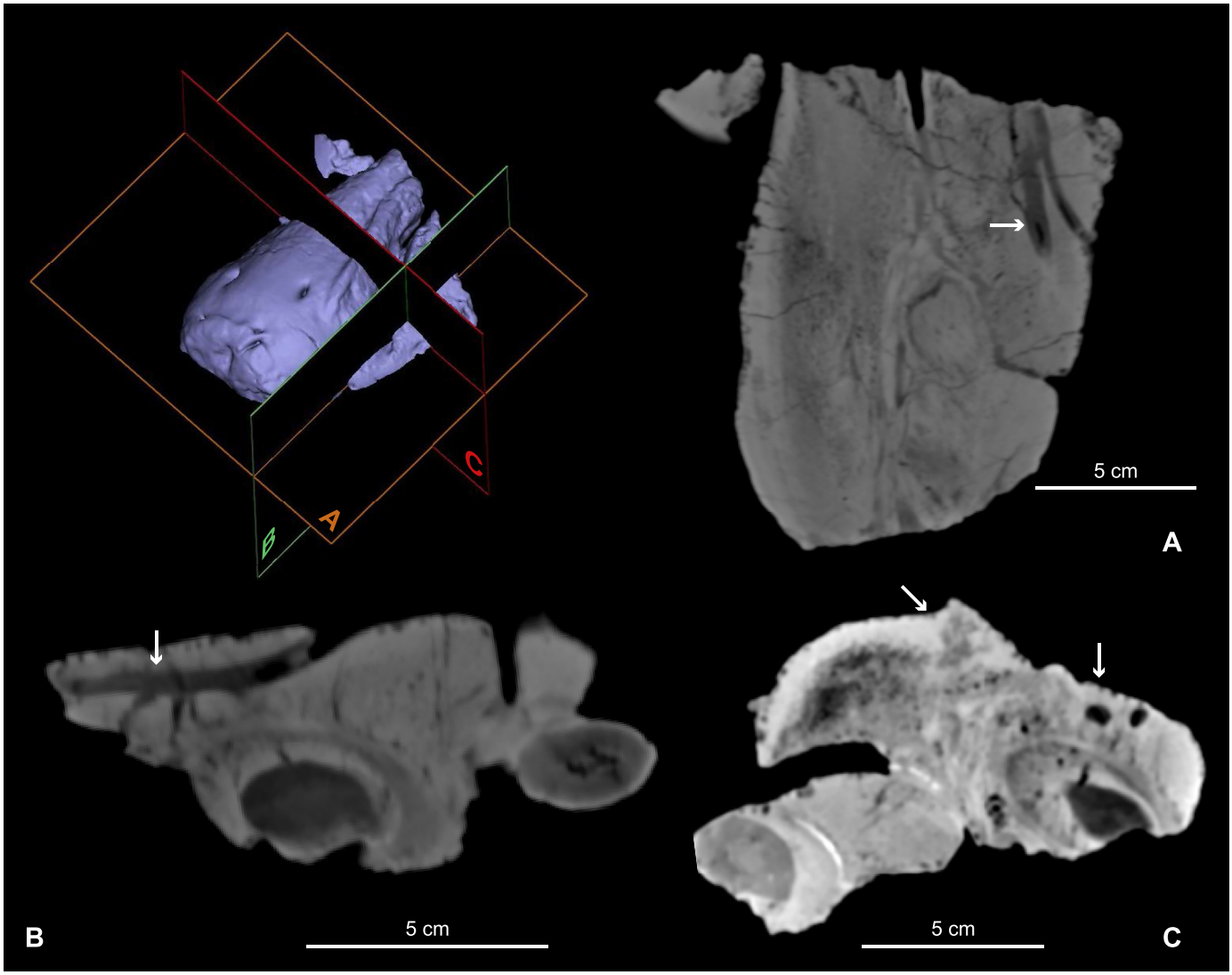

Fig. 6. cf. *Prognathodon* cf. *sectorius* NHMM 2012 072 anterior upper jaw fragments, in (**A**) coronal, (**B**) sagittal, and (**C**) axial view. Channels visible extending anteroposteriorly and dorsoventrally coagulating into a larger canal (arrows A-B, and right arrow C). Notice the difference between the neurovascular canals of the figure above in which the borders are sharply defined, and those of the larger catchment area of the maxillary canals in this figure, which are rather smudged. These maxillary canals display both different shapes, sizes and orientation when compared to the regular neurovascular cavities. The left arrow in (C) indicates the triangular radiolucency underlying the ridge-like structure.

bone (Fig. 8C, D). This subcortical structure extends posteriorly throughout the premaxillary, only to be restricted by the edge of the fossil as preserved. The maximum subcortical extent of the irregular architecture located anteriorly is nearly 2.5 cm and shallows posteriorly to just over 1 cm at its posterior edge.

The lateral extent of this anomalous structure, as measured, is roughly 18–22 mm; dorsoventrally, this is only near 9 mm.

In ventral view (Fig. 8C), the contours of the anomaly show two sharp ridges parallel to one another and separated only by a minor dip. These ridges become posteriorly less distinct. In general, lateral broadening is observed dorsally before reducing again, producing a very rough diamond-shape (Fig. 8D). The overall anomaly is oriented laterally to the left, under an angle of 50–70° to the dorsoventral plane (Fig 8A).

By comparing the tubular structures in the subsurface beneath the oblong holes in the left maxillary (Fig. 9B) with the regularly-spaced neurovascular canals (Fig. 9C), the underlying nature of the former can be resolved. The vascular network underlying the premaxillary is made up of two central tubules that run anteroposteriorly, regularly interrupted by dorsally and anterodorsally extending offshoots connecting to the neural foramina visible on the external surface of the premaxilla. These (central) tubules are parallel to one another, the distance in between the dorsal extensions are more or less equal, the width of each canal appearing consistent throughout their anteroposterior extent, and the two sets of tubules do not interconnect with their counterparts into one central canal as is the case in the subcortical maxillary canals. The set of maxillary tubules has a significantly different overall architecture and size in comparison to the neurovascular structures present in the premaxillary. The three dorsolaterally extending tubules, connected to the three oblong holes present on the exterior, have diverging widths and lengths. Major structural differences are: (1) size differences of the individual maxillary canals; (2) the three maxillary canals all converge into a central canal, that measures more than three times the size of the neurovascular structures; (3) the dorsolateral tubules all coalesce laterally from different angles and at different positions to the large central cavity, very much unlike the highly organised structure of the premaxillary neuroarchitecture. An additional zone of radiolucency surrounding the first maxillary tooth base is identified, which was

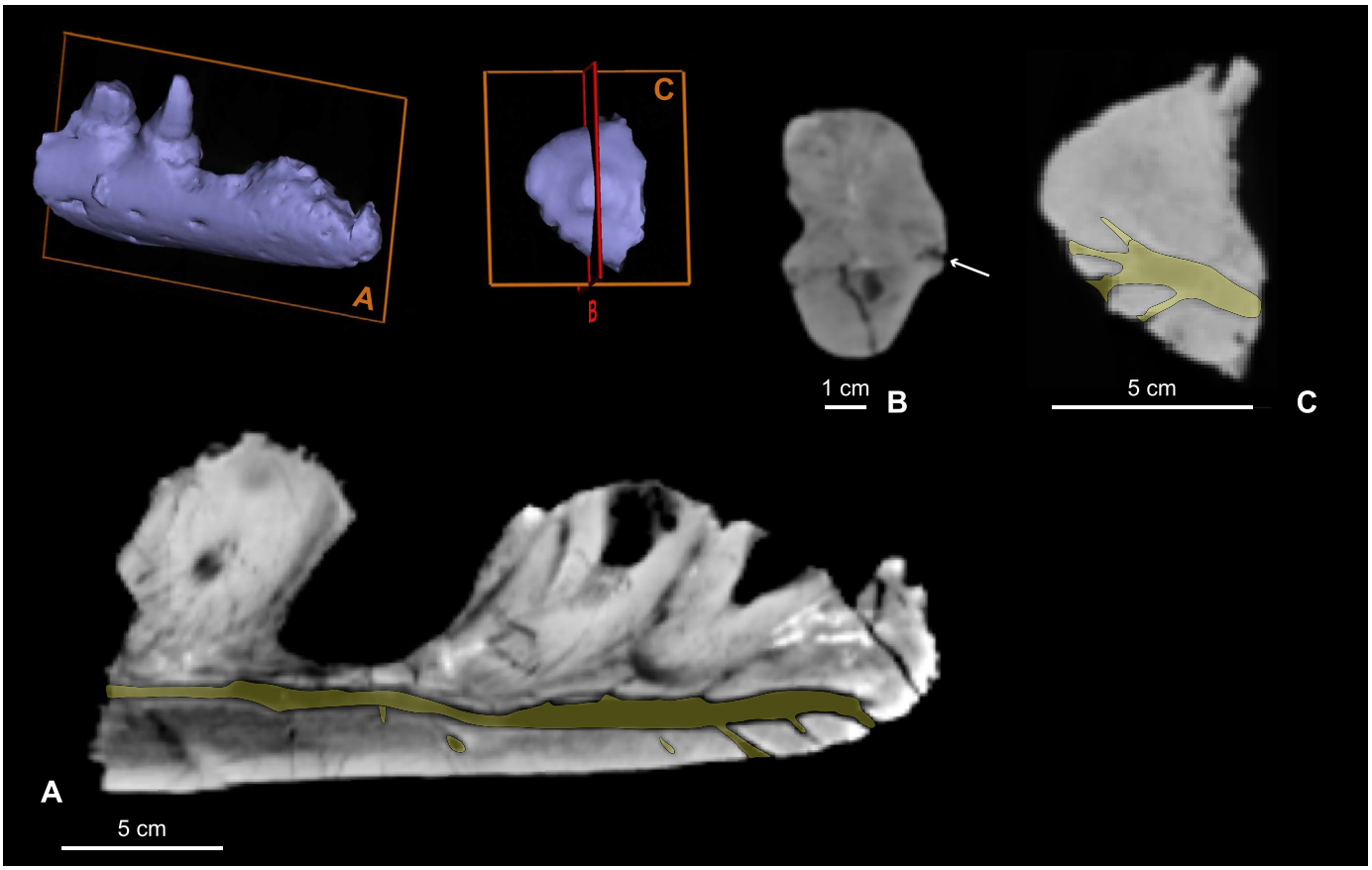

Fig. 7. cf. *Prognathodon* cf. *sectorius* CT slices of right (**A**) and left (**B, C**) dentary fragments NHMM 2012 072, in sagittal (**A, C**) and coronal (**B**) view. (**B**) Notice the radiolucent cleft centered in the protruding bony callus on the lateral surface of the dentary extending roughly seven millimeters into the bone (arrow). The semicircular radiolucency internally represents the neurovascular canals indicated in (**C**). The adjacent fracture lines most likely represent post-depositional damage (**B**). Remnants of the anteriormost tooth are visible dorsally in the sagittal view of the left dentary fragment, together with the neurovascular channels with the foramina projecting anteroventrally (**C**). For comparison (**A**), the regular structure of the branching pattern of the right dentary fragment, extending dorsally towards the teeth and anteroventrally to the foramina on the anteriormost exterior surface.

externally enclosed by irregular surface textures, and seems to be connected to the central canal of the maxillary. These features suggest that the structures visible in the subsurface of the left maxillary do not represent neurovascular structures. Although comparisons to extant savannah monitor lizards seem to corroborate the absence of neurovascular structures with external foramina in this area in the "normal" non-pathological condition, the possibility of these representing modified pre-existing neurovascular structures cannot be ruled out (Fig. 10).

4. Discussion

4.1. Distribution of lesions: pathological vs non-pathological

The similarities in extent, location and degree of healing of the anomalous bony structures on the anterior side of the upper jaw strongly suggest a common origin. The extensive damage to the anteriormost section of the premaxillary is characterised by significant loss of bone density, in comparison to the other surrounding structures. Although *post-mortem* erosion and differential mineralisation in the fossilisation process cannot be entirely ruled out as a possible cause, the elevated anterior edge of the premaxillary makes a traumatic nature likely. This 'edge' of the premaxillary is possibly related to the 2-cm-wide depression centred in the rugose area anteriorly, and the lesion interconnected to the neural canal on the dorsal surface.

Since most of the damage is located on the left side of the skull, and the majority of the *post-mortem* (e.g. bacterial) erosion is restricted to the right lateral side, it is therefore unlikely to have been the underlying cause of the density loss on the premaxillary and left maxillary. Furthermore, the dense compact bone is still present even in areas on the right lateral side that were subject to much (bacterial) erosion. This indicates that bacterial erosion could not have been the cause of the large quantity of dense bony material on the left lateral side of the skull.

4.2. Trauma: bite mark?

The shape of the anteroposteriorly oriented ridge on the premaxilla is reminiscent of a tooth strike lesion (Fig. 8C), similar to what has been reported in extant crocodilians and late Mesozoic theropod dinosaurs (Tanke and Currie, 1998, . 4; Drumheller & Brochu, 2004, 2-3). The shape and size of the subsurface anomaly that underlies this ridge, resembles a point of entry by the deepest surface penetration and a shallowing upwards at the other end. The infill that was produced of this anomaly displayed on its ventral surface a sharp bifurcating line, ragged edges, and a strong inclination at its base. Together with the posterior shallowing of this anomaly, this suggests a sharp object having been forced into the compact bone from the left lateral side, under an angle of 50–70° to the dorsoventral plane, and to a depth of nearly 25 mm deep at its maximum penetration. Subsequently, this object would have been

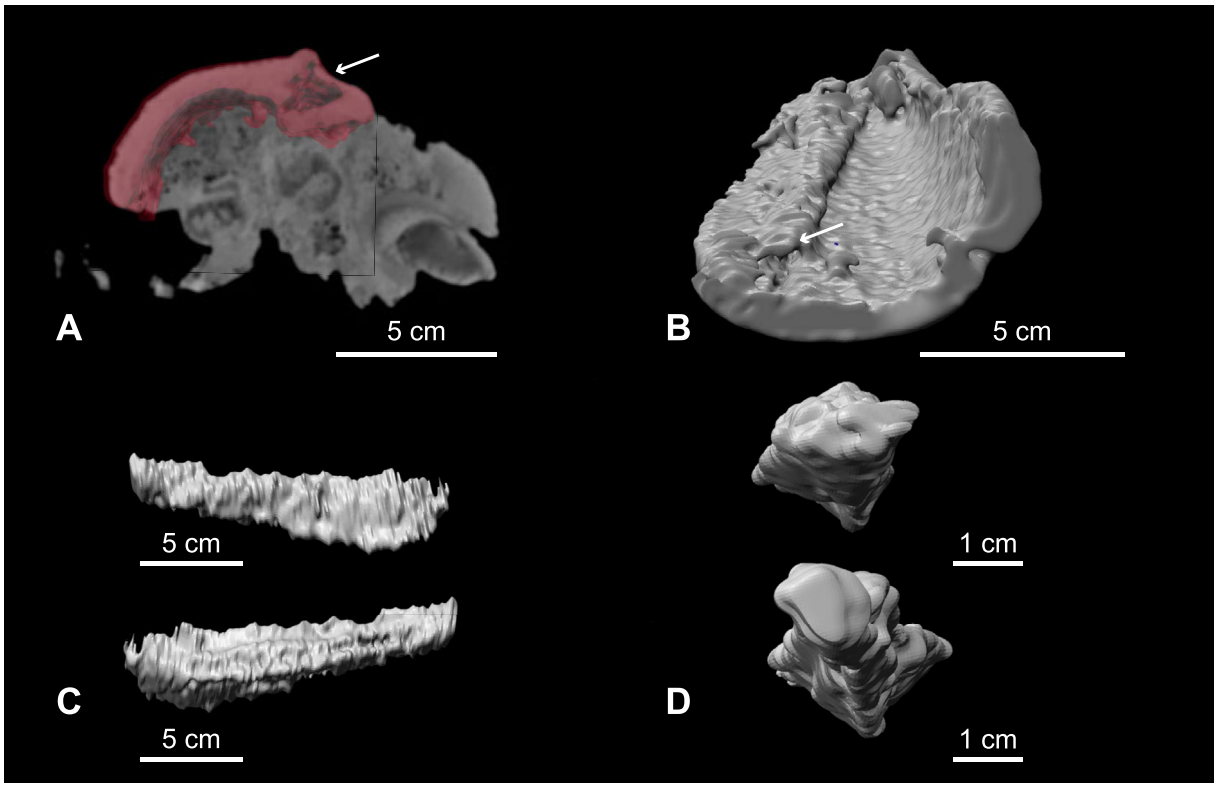

Fig. 8. *Prognathodon* cf. *sectorius* cortical bone thickness of the premaxillary of NHMM 2012 072, (**A**) in axial view. Notice variation in the thickness of the outer highly dense bone layer from the right lateral edge of the premaxillary to the left, and the adjacent anteroposteriorly extending ridge-like exostosis. The area of reduced thickness is restricted to the area underneath the ridge, suggesting that significant density changes and the exostosis share a common origin (cutoff value bone of normal density >900 HU, and abnormal bone <<900 HU). (B) anteroventral view of the compact bone layer of NHMM 2012 072, and the infill of the triangular-shaped anomaly located underneath the ridge-like exostosis of the premaxilla in (**C** above) right lateral, (**C** lower) ventral, and (**D** upper) anterior and (**D** lower) posterior view respectively. Notice that the subcortical structures are restricted to the area underneath the premaxillary anteroposterior ridge. Furthermore, the thickness of the triangular infill is consistent with a point of entry or deeper surface penetration anteriorly (C upper, right side) and a shallowing upwards posteriorly (C upper, left). In ventral view, a single or double central midline can be distinguished, and with the extent of the infill becoming wider dorsally. This pattern too is very reminiscent of a drag mark, possibly involving a sharp object penetrating the cortical bone layer e.g. Peterson et al. (2009). Notice that the dimensions and shape of the subcortical infill matches that of mosasaur teeth. More specifically, the dimensions correspond with teeth from a mosasaur that rivalled specimen NHMM 2012 072 in size or possibly slight exceeded it.

dragged in a posterior direction (as it becomes progressively shallower), projecting only several millimetres up to one centimetre downwards below the normal cortical bone layer (the added height of the ridge not taken into account). The dimensions of this lesion correspond well to the size of an isolated tooth of the same individual that is found associated, being little over one centimetre wide at the top, nearly twice that at the tooth base, and nearly 45 mm in length. This may be a good reflection of the size of the dentition of the perpetrator.

4.3. Trauma: fracture

The bony callus, or periostal bone apposition on the lateral side of the left dentary fragment could be related to the damage on the left side of the upper jaw. However, the origin of this type of damage is rather ambiguous. A swelling or 'callus' is deposited by the periost, and may be a reaction to infection, cancer, irritation, or the result of a normal fracture-healing process (compare Schulp et al., 2004 for discussion in mosasaurs). This callus is very likely the result of localised trauma, as a clear puncture can be seen in the centre. Normal fracture healing involves the increase of periosteal and medullary blood supply, followed by infilling of the fracture by highly vascular fibrous callus. The exterior of the callus seems to have started uniting the fractured surfaces with bony tissue, suggesting a relatively advanced state of healing (Rothschild and Martin, 1993, 2006). The presence of a callus with various reparative tissues indicates that the organism survived the initial facial injury for at least several weeks (Rothschild and Martin, 2006; Xing et al., 2018).

4.4. Traumatic-infectious/bacterial infection and the mosasaur immune system

The oblong lesions on the maxillary and lateral side of the exostosial ridge on the premaxillary, together with the disrupted bone surface with extensive pitting, might hint at a bacterial infection subsequent to initial rostral trauma sustained. Extant and fossil crocodylians, often used as an analogue for mosasaur behaviour, frequently display deep facial wounds that penetrate bone, and those wounds often become a point of entrance for a variety of bacterial agents (e.g. Mackness and Sutton, 2000; Avilla et al., 2004; Wolff et al., 2009; Martin, 2013). The vascular structures in the subsurface of the maxilla connecting the lesions into a single wide canal, are not unlike the radiolucent endosteal changes associated with the abscess cavities of pyogenic osteomyelitis (i.e. pus-generating bone infection) as observed in mammals (And and Castello, 1995; Ortner and Putschar, 2003; Divers and Mader, 2005; Rothschild and Martin, 2006; Silverman, 2006; Jadwiszczak and Rothschild, 2019). Another indication for osteomyelitis with an exogenous cause might be the sclerotic margins lateral to the ridge and in-between the plate-like cortical bone structures of the premaxillary and maxillary respectively (Rothschild and Martin, 2006).

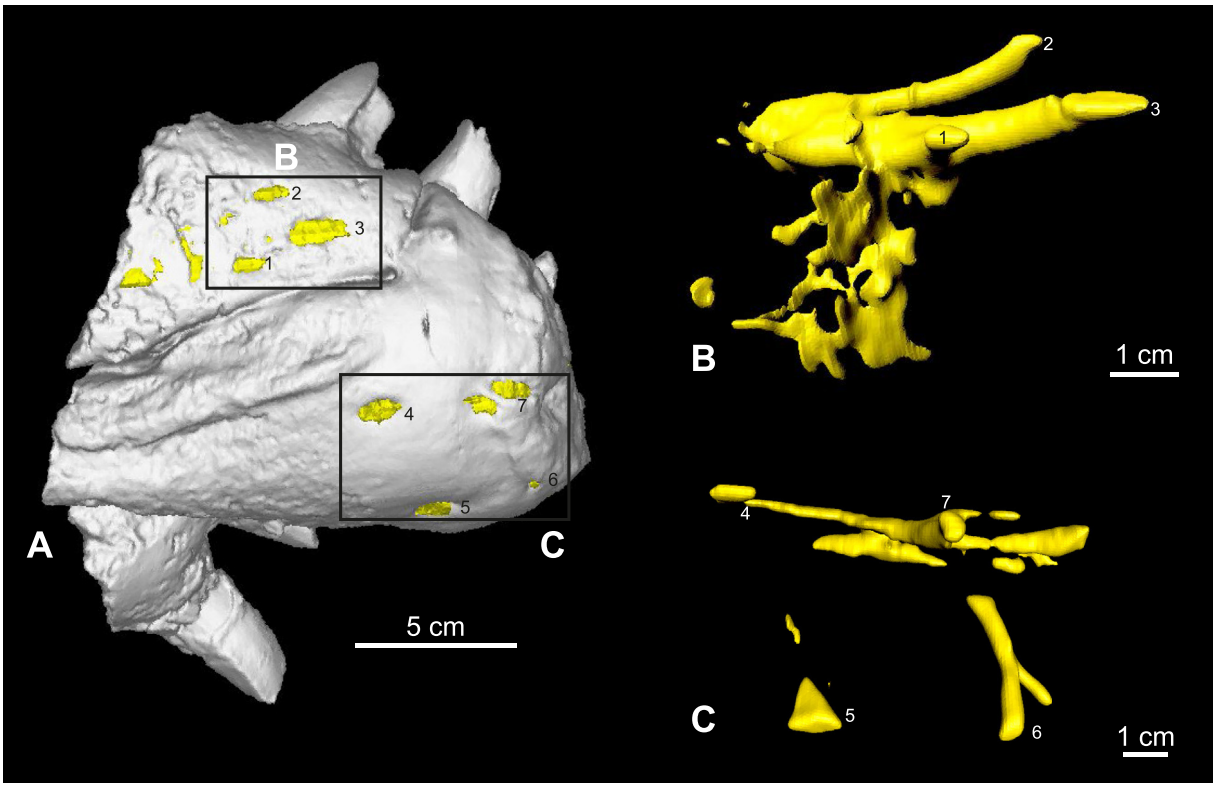

Fig. 9. *Prognathodon* cf. *sectorius* NHMM 2012 072 (**A**); a 3D reconstruction of the infill underlying the three oblong lesions in dorsolateral view (**B**); and an infill of the regularly spaced neurovascular canals present in the premaxilla (C). Notice the difference in both size and architecture. First off, the width differs significantly between the two structures. Furthermore, the neurovascular structures all join dorsally into two central canals. The structures on the maxillary all join laterally into a single structure. The highly irregular structures adjacent to the three maxillary canals surround the first maxillary tooth base. Together these features suggest that the structures in the maxillary do not represent neurovascular structures or possibly modified pre-existing canals. (cut-off values were established with bone of normal density represented by > 800 HU; radiolucent abnormal bone regions of <800 HU giving additional resolution required for a continuous, uninterrupted 3D representation).

The failure of the soft tissue and the newly produced bone to isolate the infection likely led to extensive spreading, which initiated even more osteoblastic activity. The increased intraosseous pressure of infection-induced inflammations may have interfered with vascular supply, causing tissue necrosis and exposing underlying trabecular bone (Rothschild and Martin, 1993, 2006; Ortner and Putschar, 2003). Although relatively little is known about the innate and adaptive immune system of reptiles, and even contradictory observations have been made, their response to infection differs in some ways from that of mammals (Huchzermeyer and Cooper, 2000; Silverman, 2006; Stacy and Pessie, 2007; Zimmerman et al., 2010, p. 661). Overall, the secondary periosteal, cortical and endosteal response to infection is less prominent in reptiles than in mammals (Silverman, 2006). In fact, reptiles do not produce liquid exudates (i.e. pus), which is a typical mammalian response (Stacy and Pessie, 2007; Zimmerman et al., 2010). Instead reptiles generally produce solid aggregates of degenerated heterophils, termed caseous granulomas or fibriscesses, soon (<7 days) after extracellular infection, eventually turning chronic on the long term (Huchzermeyer and Cooper, 2000; Stacy and Pessie, 2007; Zimmerman et al., 2010; Anné et al., 2015). In short, when triggered, the innate immune system of reptiles produces non-specific white blood cells (heterophilic leukocytes), which contain the infection by forming a solid mass of 'dead' heterophils within the tissue (Huchzermeyer and Cooper, 2000; Stacy and Pessie, 2007; Zimmerman et al., 2010). The difference between heterophils of extant reptiles and the roughly analogous neutrophils of mammalian immune systems is translated into the production of a solid granuloma in the former and the production of fluid pus in the latter group (Stacy and Pessie, 2007; Zimmerman et al., 2010; Huchzermeyer and Cooper, 2000). What is interesting to note is that the tubular architecture of the maxillary lesions and the suppurative-like appearance of the subcortex in the present mosasaur individual seems to be more closely comparable to pyogenic osteomyelitis of mammals than the granulomatous response of reptiles. The infecting bacteria may have used pre-existing neurovascular structures similar to those existing in the anterior part of the premaxilla to spread and eventually drain the infectious material, possibly even becoming chronic or systemic osteomyelitis. On the other hand, some of these structures in the subsurface may have been created solely by the pyogenic bacteria and thus represent osteolytic canals for draining the abscesses associated with the large infectious area (e.g. as documented in Reisz et al., 2011). The architecture of the subsurface structures in the maxillary favours the latter explanation, as these are highly irregular in size and shape and do not display the same distribution of canals, nor do they interconnect in a similar fashion as seen in neurovascular structures. Furthermore, no canals in such orientation and size have been identified by external observation of other (*Prognathodon*-like) mosasaurs, nor of any related extant taxa (collections of NHMM, Fig. 10 here and e.g., Kass, 1999; Schulp et al., 2008; Lindgren and Schulp, 2010; Konishi et al., 2011; Grigoriev, 2013). Although a degree of soft tissue involvement seems very likely, it is unclear if these osteolytic canals were associated with extensive soft tissue abscesses or not.

4.5. Traumatic origin: violent interactions?

The shape of the anteroposteriorly oriented ridge-like lesion, the structure of the subcortical anomaly, the location and extent of

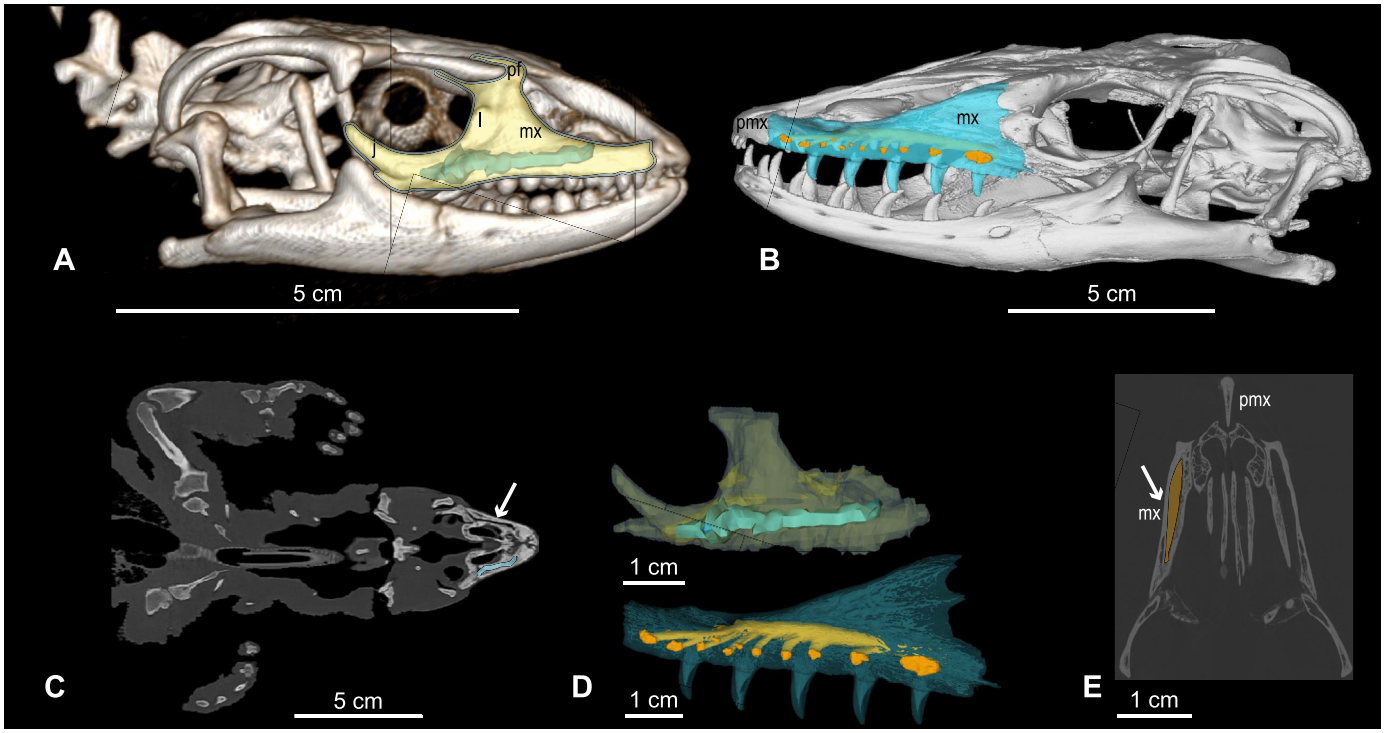

Fig. 10. Comparison of the premax-maxillary complex of cf. *Prognathodon sectorius* NHMM 2012 072, to that of extant monitor lizards. (**A-B**) the anterior skull morphology and architecture as can be observed in the extant savannah monitor lizard (*Varanus exanthematicus*) and the Asian water monitor (*Varanus salvator*, PIMUZ A/III 1493) in right and left lateral view, respectively. (**C**) radiograph (above) and three-dimensional reconstructions (**D**) in right lateral and left view (**E**) the same region visualized in the before-mentioned species of Asian water monitor lizard in dorsal view. Notice, no multituberal structures with irregular spacing or distribution similar to those in NHMM 2012 072 representing neurovascular canals can be distinguished in the maxillary or anterolateral exterior of the upper jawbones of the savannah monitor lizard (*Varanus exanthematicus*) and the Asian water monitor (*Varanus salvator*). Seemingly confirming this observation, based upon the radiological imagery no endosteal analogues to the heavily branched tubular structures are present in this species of extant monitor lizards. These observations concur with the diagnosis of these endosteal architectural features as reflecting the prolonged effects of chronic pyogenic osteomyelitis. Data for the extant *Varanus exanthematicus* is from Schachner et al. (2013). Abbreviations: j = jugal; l = lacrimal; mx = maxillary; pf = prefrontal; and pmx = premaxillary.

the damage on both the maxillary, premaxillary and possibly the left dentary, together with the subsequent healing processes, all indicate a traumatic origin of these pathologies, and are most parsimoniously explained by a not immediately lethal interaction with one (or more) large mosasaur(s). Cranial lesions have previously been noted in mosasaurs including reports from the Maastrichtian type section (Lingham-Soliar, 1998, 2004; Mulder, 1999; Schulp et al., 2004, 2006, 2013). Testifying to the aggressive interactions between mosasaurs, a multitude of injuries have been suggested as evidence, such as puncture wounds to the posterior side of the skull, anterior side of the upper jaw and lateral side of the mandibles (e.g. Williston, 1898; Bell and Martin, 1995; Lingham-Soliar, 1998, 2004; Mulder, 1999; Schulp et al., 2004, 2006; Everhart, 2008). The earliest postulation for inter- or intraspecific behaviour in mosasaurs can be traced back to Williston (1898, p. 214), who observed, '... exostosial growth in their lower jaws, the vertebrae, especially those of the tail, and in the paddles, especially the digits." The distribution of these exostosial growths has been described in more detail in recent years, and can be attributed to a variety of causes including infectious spondylitis, diffuse idiopathic skeletal hyperostosis (DISH, or non-pathological 'tendon ossification'), traumatically-induced osteomyelitis, and normal fracture healing (Schulp et al., 2004, 2006). Direct and especially unambiguous evidence of interactions between mosasaurs, however, is extremely rare and thus the present specimen offers an extraordinary opportunity to reconstruct in more detail one such interaction.

Considering the size of the victim, which is reconstructed to have been well in excess of ten metres body length, and the shape of the suspected tooth-strike lesion, the only plausible attacker with sufficient bite force to penetrate the cortical bone to such an extent is another mosasaur (Lingham-Soliar, 1998). Estimates of the dimension of the aggressor seem to approach those of the victim, or possibly even slightly exceed them, meaning in excess of ten metres. Extant crocodiles display a snout-grappling behaviour during the mating season, while protecting territory, or in intraspecific competition over potential mates (Lingham-Soliar, 1995, 1998, 2004; Tanke and Currie, 1998; Peterson et al., 2009). This behaviour has been postulated for mosasaurs in multiple cases of facial lesions (Bell and Gordon in Monastersky, 1989; Rothschild and Martin, 1993, 2006; Bell and Martin, 1995; Lingham-Soliar, 1998, 2004; Mulder, 1999; Schulp et al., 2004, 2006; Everhart, 2008) and a semi-lateral grappling attack would certainly explain the tooth-strike mark and adjacent damage to the maxillary.

4.6. Survival time

The estimated survival time for this particular individual may have ranged from a few weeks to a couple of months at least. The extensive bone remodelling and the state of healing could have occurred within several weeks after the sustained injury, as fibrocartilagenous callus formation generally takes place within two or three weeks in humans and resorption occurs over a period of sixteen weeks under normal conditions (Rothschild and Martin, 1993, 2006; Lingham-Soliar, 2004). As far as bone repair is concerned, a major difference between birds and mammals on the one hand, and lizards and amphibians on the other concerning bone repair, is that the latter do not produce secondary cartilage.

Therefore, the bony callus present is not comprised of rapidly produced cartilaginous precursor material. Rather, endosteal new bone forms slowly and is present after three weeks, setting a relatively high minimum survival time for this organism (Rothschild and Martin, 1993; Lingham-Soliar, 2004). However, the rate of repair could be significantly decreased and thus the survival time markedly extended, by the influence of infections or disease, as this is a reflection of the overall health of the organism (Lingham-Soliar, 2004).

The negative effects of the infection associated with the trauma could have contributed to the eventual death of this individual. It appears that the infection was still ongoing at the time of death, and possibly even starting to extend to the first maxillary tooth base.

5. Conclusions

Specimen NHMM 2012 072 of *Prognathodon* cf. *sectorius* suffered various injuries that are visible on the anterior sections of the premaxillary, left maxillary and left dentary, likely from an encounter with one or more mosasaur(s). Other large predators including sharks, rare crocodilians (e.g. *Thoracosaurus* and others) and elasmosaurids can be excluded or are deemed very unlikely as based on the morphology of the lesions, their rare occurrence in the area, or the lack of adequate bite force (Mulder, 1998; Mulder et al., 1998, 2000, 2016). The force of the trauma was concentrated on the left lateral side of the skull, approaching from an angle of 50–70° to the dorsoventral plane. This allowed for the teeth to penetrate the premaxillary and maxillary, as well as the left dentary at the same instance. It appears that one but likely more teeth dragged through the compact bone layer covering the premaxillary, resulting in an anteroposteriorly-oriented gouge, later forming a ridge-like exostosis. This may be due to movement of the victim relative to the attacker(s), resulting in multiple parallel scrapes in the subsurface of the premaxillary as the attacker's teeth dragged across its surface. The concentrated force of the bite resulting in a localised fracture in the left dentary, eventually leading to the formation of a reparative bony callus. Additional damage to the anterior part of the premaxilla may also be indicative of a bite resulting in the amputation of its anteriormost section, and obscuring of the first tooth position on both sides by bone reparative processes. Only portions of the premaxillary and maxillaries are preserved, the absence of the internarial bar and large portions of the maxillary obscure more details of this violent interaction. It is clear that this mosasaur survived the encounter and very likely persisted for a significant time. However the resulting infectious processes may have hampered the healing processes, while at the same time spreading throughout the premaxillary and maxillary. As a result, a vast amount of bone is dissolved in the maxillary, creating multiple anteroposteriorly oriented tubules and even starting to affect the enamel of the first maxillary tooth base. The underlying nature of such an encounter between two (or more) proportionally similar mosasaurs is highly speculative. However, the identification of more such encounters in the fossil record, suggests either intra- or interspecific competition or predation. According to the size of the victim and the suggested attacker(s), the latter would appear unlikely.

The Maastrichtian type locality is home to five species of four different genera of mosasaur, including *Carinodens belgicus* (~3 m in length), *Plioplatecarpus marshi* (~5–6 m), and the larger *Prognathodon sectorius* (>8 m), *Prognathodon saturator* (~12 m) and *Mosasaurus hoffmanni* (14–17 m), although not all taxa have been reported from the lower stratigraphic reaches where NHMM 2012 072 was discovered (Mulder, 1999 and references therein; Jagt et al., 2008; Schulp et al., 2008, 2013). As an analogy for mosasaur behaviour, extant crocodilians are often proposed. During mating season, while protecting territory, or directly during intraspecific competition, extant crocodilians engage in display behaviour ('head-slapping') or in grappling behaviour (Peterson and Vittore, 2012). These encounters often result in serious injuries, even partial or complete amputations of limbs and jaw sections have been noted, but such encounters are rarely lethal (Wolff et al., 2009). Crocodilians and lizards have strong immune systems that enabled them to deal with the resulting infections (Lingham-Soliar, 2004). The immune system of snakes, although representing largely unexplored terrain, seems to work largely similar to that of mammals, although there are some important differences (Stacy and Pessie, 2007; Zimmerman et al., 2010). Reptiles generally exhibit a stronger innate system response (Stacy and Pessie, 2007; Zimmerman et al., 2010). The innate immune response of ectotherms also produces a body temperature increase, albeit not physiologically but behaviourally, this makes the immune response of ectotherms relatively dependent on the environmental conditions (Stacy and Pessie, 2007; Zimmerman et al., 2010). Another difference is that, in contrast to mammals, the reptilian inflammatory response does not produce a liquid pus exudate but rather a 'cheese-like' (i.e. caseous) mass of fibrous tissues (a fibriscess) (Peterson and Vittore, 2012; Zimmerman et al., 2010; Stacy and Pessie, 2007). Mosasaurs may further differ in that they may have reached a degree of giganto- or endothermy, and therefore extant ectothermic reptilians may not present the ideal immunological models for these marine reptiles.

Mosasaurs would have had strong immune systems similar to those of extant reptilians, as the extent of the injuries did not result in immediate death of this specimen. Interestingly, mosasaurs appear to differ in some respects as the canals in the subsurface of the maxilla seem to hint at a liquid pus rather than typical reptilian caseous growths. Eventually the demise of this mosasaur seems to have preceded the complete healing of these injuries, as reparative processes were still ongoing at the time of death. The exact cause of death cannot be determined with certainty; however, since the infection seems to have still been ongoing at the time of death, the chronic infection and potentially reduced feeding capability may have contributed to the eventual death of this animal. This case study illustrates the great potential of integrative three-dimensional approaches in palaeopathological studies to provide a much more comprehensive and detailed description of alterations and underlying physiological processes. Ideally pathological studies should aim to incorporate both histological and radiological techniques (including 3D-visualizations) to supplement traditional external morphological descriptions as suggested by previous authors (e.g. Straight et al., 2009; Peterson and Vittore, 2012; Anné et al., 2015; Hedrick et al., 2016). This allows for a much higher degree of certainty in identifying a causative factor, as well as providing a much more detailed description of skeletal processes on a tissue level.

CRediT authorship contribution statement

Dylan Bastiaans: Conceptualization, Data curation, Formal analysis, Investigation, Methodology, Software, Validation, Writing - original draft, Writing - review & editing. **Jeroen J.F. Kroll:** Data curation, Methodology, Validation, Resources, Writing - review & editing, Visualization. **Dirk Cornelissen:** Validation, Investigation, Writing - review & editing. **John W.M. Jagt:** Validation, Resources, Writing - review & editing, Supervision. **Anne S. Schulp:** Conceptualization, Validation, Resources, Writing - review & editing, Visualization, Supervision.

Acknowledgements

We owe many thanks to Ernst Smid and the radiology and radiotherapy department of the University Medical Centre Utrecht (UMC, Utrecht, the Netherlands) and the forensic radiology department of the Maastricht University Medical Centre (MUMC+, Maastricht, the Netherlands) for providing the opportunity to scan the dentary and the premaxillary-maxillary section of the upper jaw of the mosasaur, respectively, and helpful comments concerning the diagnosis. Special thanks to Thorsten Plogschties (Rheinische Friedrich-Wilhelms-Universität Bonn) for help with the various three-dimensional reconstructions (Avizo, Meshlab and Polyworks) and helpful feedback. Additional thanks to Bruce M. Rothschild, for new insights into and comments on the preliminary work as presented during the 74th Annual Meeting in Berlin (November 2014). DB was partially funded through the Swiss National Science Foundation (grant no. 31003 A_179401 to T. Scheyer). We owe much gratitude to PD Dr. Torsten Scheyer (Paläontologisches Institut und Museum, Universität Zürich) and Dr. Ashley Latimer for providing a scan of the Asian water monitor (*Varanus salvator*). Furthermore, we are grateful to PD. Dr. Torsten Scheyer and Louis Verding (NHMM, Maastricht, the Netherlands) for helpful discussions on normal and pathological appearance in histological and radiological sections. We would like to thank the former ENCI HeidelbergCement Group for support with the excavation, providing the opportunity and means to secure the specimen. Special thanks to quarry operator Carlo Brauer for having the keen eye to spot and recognise the fossil and for persuading his superiors to postpone quarrying operations at the site. Furthermore, without the dedication, professionalism and effort of all volunteers and others involved in preparation at the Natuurhistorisch Museum Maastricht (NHMM, Maastricht, the Netherlands), the present survey of this new mosasaur specimen would not have been possible. Lastly, we would like to thank Editor-in-Chief Dr. Koutsoukos and two anonymous reviewers for their constructive and helpful comments that have improved this manuscript.

References

And, M.J., Castello, H.P., 1995. Osteomyelitis of the skull in a leopard seal, *Hydrurga leptonyx*. Marine Mammal Science 11, 403–406.

Anné, J., Garwood, R.J., Lowe, T., Withers, P.J., Manning, P.L., 2015. Interpreting pathologies in extant and extinct archosaurs using micro-CT. PeerJ 3, 1–14.

Avilla, L.S., Fernandes, R., Ramos, D.F., 2004. Bite marks on a crocodylomorph from the Upper Cretaceous of Brazil: evidence of social behavior? Journal of Vertebrate Paleontology 24, 971–973.

Bell Jr., G.L., Barnes, K.R., 2007. First record of stomach contents in *Tylosaurus nepaeolicus* and comments on predation among Mosasauridae. In: Everhart, M. (Ed.), Proceedings of the Second Mosasaur Meeting, vol. 3, pp. 9–10. Fort Hays Studies Special Issue.

Bell Jr., G.L., Martin, J.E., 1995. Direct evidence of aggressive intraspecific competition in *Mosasaurus conodon* (Mosasauridae: Squamata). Journal of Vertebrate Paleontology 15 (Suppl. 3), 18A.

Bell, P.R., 2010. Palaeopathological changes in a population of *Albertosaurus sarcophagus* from the Upper Cretaceous Horseshoe Canyon Formation of Alberta, Canada. Canadian Journal of Earth Sciences 47, 1263–1268.

Bell, P.R., Currie, P.J., 2010. A tyrannosaur jaw bitten by a confamilial: scavenging or fatal agonism? Lethaia 43, 278–281.

Divers, S.J., Mader, D.R., 2005. Reptile Medicine and Surgery. Elsevier Health Sciences, Amsterdam, pp. 1–1264.

Dollo, L., 1882. Note sur l'ostéologie des *Mosasauridae* [sic]. Bulletin du Musee Royal d'Histoire Naturelle de Belgique 1, 55–74.

Dortangs, R.W., Schulp, A.S., Muler, E.W.A., Jagt, J.W.M., Peeters, H.H.G., de Graaf, D.Th, 2002. A large new mosasaur from the Upper Cretaceous of The Netherlands. Netherlands Journal of Geosciences 81, 1–8.

Drumheller, S.K., Brochu, C.A., 2014. A diagnosis of *Alligator mississippiensis* bite marks with comparisons to existing crocodylian datasets. Ichnos 21, 131–146.

Einarsson, E., Lindgren, J., Kear, B.P., Siverson, M., 2010. Mosasaur bite marks on a plesiosaur propodial from the Campanian (Late Cretaceous) of Southern Sweden. Geologiska Föreningens Förhandlingar (GFF) 132, 123–128.

Everhart, M.J., 2008. A bitten skull of *Tylosaurus kansasensis* (Squamata: Mosasauridae) and a review of mosasaur-on-mosasaur pathology in the fossil record. Transactions of the Kansas Academy of Science 111, 251–262.

Everhart, M.J., 2012. Oceans of Kansas. "Mosasaur Pathology: Even the big guys got no respect. http://oceansofkansas.com/mosapath.html.

Foth, C., Evers, S.W., Pabst, B., Mateus, O., Flisch, A., Patthey, M., Rauhut, O.W., 2015. New insights into the lifestyle of *Allosaurus* (Dinosauria: Theropoda) based on another specimen with multiple pathologies. PeerJ 3, 1–33 e940.

Gaudry, A., 1890. Les enchaînements du monde animal dans les temps géologiques: fossiles secondaires. Librairie F. Savy, Paris), pp. 1–323.

Grigoriev, D.V., 2013. Redescription of *Prognathodon lutugini* (Squamata, Mosasauridae). Proceedings of the Zoological Institute RAS 317, 246–261.

Hanna, R.R., 2002. Multiple injury and infection in a sub-adult theropod dinosaur *Allosaurus fragilis* with comparisons to allosaur pathology in the Cleveland-Lloyd dinosaur quarry collection. Journal of Vertebrate Paleontology 22, 76–90.

Hedrick, B.P., Gao, C., Tumarkin-Deratzian, A.R., Shen, C., Holloway, J.L., Zhang, F., Hankenson, K.D., Liu, S., Anné, J., Dodson, P., 2016. An injured *Psittacosaurus* (Dinosauria: Ceratopsia) from the Yixian Formation (Liaoning, China): Implications for *Psittacosaurus* Biology. The Anatomical Record 299, 897–906.

Huchzermeyer, F.W., Cooper, J.E., 2000. Fibriscess, not abscess, resulting from a localised inflammatory response to infection in reptiles and birds. The Veterinary Record 147, 515–516.

Jadwiszczak, P., Rothschild, B.M., 2019. The first evidence of an infectious disease in early penguins. Historical Biology 31, 177–180.

Jagt, J.W.M., Jagt-Yazykova, E.A., 2012. Stratigraphy of the type Maastrichtian-a synthesis. Scripta Geologica - Special Issues 8, 5–32.

Jagt, J.W.M., Cornelissen, D., Mulder, E.W.A., Schulp, A.S., Severijns, J., Verding, L., 2008. The youngest *in situ* record to date of *Mosasaurus hoffmanni* (Squamata, Mosasauridae) from the Maastrichtian type area, the Netherlands. In: Everhart, M. (Ed.), Proceedings of the Second Mosasaur Meeting, vol. 3. Fort Hays Studies Special Issue, pp. 73–80.

Kass, M.S., 1999. *Prognathodon stadtmani*:(Mosasauridae) a new species from the Mancos Shale (lower Campanian) of western Colorado. Vertebrate Palaeontology in Utah 99–1, 275–294.

Keutgen, N., 2018. A bioclast-based astronomical timescale for the Maastrichtian in the type area (southeast Netherlands, northeast Belgium) and stratigraphic implications: the legacy of P.J. Felder. Netherlands Journal of Geosciences 97, 229–260.

Konishi, T., Brinkman, D., Massare, J.A., Caldwell, M.W., 2011. New exceptional specimens of *Prognathodon overtoni* (Squamata, Mosasauridae) from the upper Campanian of Alberta, Canada, and the systematics and ecology of the genus. Journal of Vertebrate Paleontology 31, 1026–1046.

Kruytzer, E.M., 1957. De *Mosasaurus* van Bemelen. *Mosasaurus hoffmanni* Mantell. Natuurhistorisch Maandblad 46, 125–127.

Lindgren, J., Schulp, A.S., 2010. New material of *Prognathodon* (Squamata: Mosasauridae), and the mosasaur assemblage of the Maastrichtian of California, USA. Journal of Vertebrate Paleontology 30, 1632–1636.

Lingham-Soliar, T., 1995. Anatomy and functional morphology of the largest marine reptile known, *Mosasaurus hoffmanni* (Mosasauridae, Reptilia) from the Upper Cretaceous, Upper Maastrichtian of The Netherlands. Philosophical Transactions of the Royal Society of London - B 347, 155–180.

Lingham-Soliar, T., 1998. Unusual death of a Cretaceous giant. Lethaia 31, 308–310.

Lingham-Soliar, T., 2004. Palaeopathology and injury in the extinct mosasaurs (Lepidosauromorpha, Squamata) and implications for modern reptiles. Lethaia 37, 255–262.

Mackness, B., Sutton, R., 2000. Possible Evidence for intraspecific aggression in a Pliocene crocodile from north Queensland. Alcheringa: An Australasian Journal of Palaeontology 24, 55–62.

Martin, J.E., 2013. Surviving potentially lethal injury? Bite mark and associated trauma in the vertebra of a Dyrosaurid crocodilian. Palaios 28, 6–8.

Martin, J.E., Bell Jr., G.L., 1995. Abnormal caudal vertebrae of Mosasauridae from Late Cretaceous marine deposits of South Dakota. Proceedings of the South Dakota Academy of Science 74, 23–27.

Martin, L.D., Rothschild, B.M., 1989. Paleopathology and diving mosasaurs. American Scientist 77, 460–467.

Meijer, A.W.F., 1985. Hoe wervelvergroeïingen een paleontoloog op het verkeerde spoor brachten. Natuurhistorisch Maandblad 74, 130–131.

Monastersky, R., 1989. A nose for combat. Science News 136, 318.

Monastersky, R., 1990. Reopening old wounds. Science News 137, 40–42.

Moodie, R.L., 1917. Studies in Paleopathology I: general consideration of the evidences of pathological conditions found among fossil animals. Annals of Medical History 1, 374–393.

Moodie, R.L., 1923. The antiquity of disease. University of Chicago Press, pp. 1–174.

Mudge, B.F., 1877. Notes on the Tertiary and Cretaceous periods of Kansas. In: Part I (Geology) of the Ninth Annual Report. U.S. Geological and Geographical Survey of the Territories (Hayden), pp. 1–827 for 1875.

Mulder, E.W.A., 1985. Beenvliesontsteking: een oude kwaal! Natuurhistorisch Maandblad 74, 129–130.

Mulder, E.W.A., 1998. Thoracosaurine vertebrae (Crocodylia; Crocodylidae) from the Maastrichtian type area -. Proceedings of the Koninklijke Nederlandse Akademie Van Wetenschappen 100, 161–170.

Mulder, E.W.A., 1999. Transatlantic latest Cretaceous mosasaurs (Reptilia, Lacertilia) from the Maastrichtian type area and New Jersey. In: Jagt, J.W.M., Lambers, P.H., Mulder, E.W.A., Schulp, A.S. (Eds.), Proceedings of the Third European Workshop on Vertebrate Paleontology (Maastricht, May 6-9, 1998), vol. 78, pp. 281–300. Geologie en Mijnbouw.

Mulder, E.W.A., 2001. Co-ossified vertebrae of mosasaurs and cetaceans: implications for the mode of locomotion of extinct marine reptiles. Paleobiology 27, 724–734.
Mulder, E.W.A., Bardet, N., Godefroit, P., Jagt, J.W.M., 2000. Elasmosaur remains from the Maastrichtian type area, and a Review of latest Cretaceous Elasmosaurs (Reptilia, Plesiosauroidea). Bulletin de L'institut Royal Des Sciences Naturelles de Belgique, Science de la Terre 70, 161–178.
Mulder, E.W.A., Jagt, J.W.M., Kuypers, M.M.M., Peeters, H.H.G., Rompen, P., 1998. Preliminary observations on the stratigraphic distribution of Late Cretaceous marine and terrestrial reptiles from the Maastrichtian type area (SE Netherlands, NE Belgium). Oryctos 1, 55–64.
Mulder, E.W.A., Jagt, J.W.M., Stroucken, J.W., 2016. New records of latest Cretaceous neosuchian crocodyliforms from the Maastrichtian type area (southern Limburg, the Netherlands). In: Sullivan, R.M., Lucas, S.G. (Eds.), Fossil Record 5. New Mexico Museum of Natural History and Science Bulletin, vol. 74, pp. 169–172.
Ortner, D.J., Putschar, W.G.J., 2003. Identification of pathological conditions in human skeletal remains. Smithsonian Contributions to Anthropology 28, 1–500. Academic Press.
Peterson, J.E., Henderson, M.D., Scherer, R.P., Vittore, C.P., 2009. Face biting on a juvenile tyrannosaurid and behavioral implications. Palaios 24, 780–784.
Peterson, J.E., Vittore, C.P., 2012. Cranial pathologies in a specimen of *Pachycephalosaurus*. PloS One 7, e36227.
Reisz, R.R., Scott, D.M., Pynn, B.R., Modesto, S.P., 2011. Osteomyelitis in a Paleozoic reptile: ancient evidence for bacterial infection and its evolutionary significance. Naturwissenschaften 98, 551–555.
Ritsema, C.J., Groenenberg, J.E., 1993. Pyrite Oxidation, Carbonate Weathering, and Gypsum Formation in a Drained Potential Acid Sulfate Soil. Soil Science Society of America Journal 5, 968–976.
Rothschild, B.M., 2013. Clawing their way to the top: Tyrannosaurid pathology and lifestyle. In: Parrish, J.M., Molnar, R.E., Currie, P.J., Koppelhus, E.B. (Eds.), Tyrannosaurid Paleobiology. Indiana University Press, Bloomington, Indiana, pp. 210–221.
Rothschild, B.M., Martin, L.D., 1987. Avascular Necrosis: Occurrence in Diving Cretaceous Mosasaurs. Science 236, 75–77.
Rothschild, B.M., Martin, L.D., 1993. Paleopathology: Disease in the fossil record. CRC Press, Boca Raton/London, pp. 1–386.
Rothschild, B.M., Martin, L.D., 2006. Skeletal Impact of Disease. Bulletin of the New Mexico Museum of Natural History and Science vol. 33, 1–226.
Rothschild, B.M., Tanke, D., 1992. Paleoscene 13: Paleopathology of Vertebrates: Insights to Lifestyle and Health in the Geological Record. Geoscience Canada 19, 73–80.
Russell, D.A., 1967. Systematics and morphology of American mosasaurs. Bulletin of the Peabody Museum of Natural History, Yale University vol. 23, 1–241.
Schachner, E.R., Cieri, R.L., Butler, J.P., Farmer, C.G., 2013. Unidirectional pulmonary airflow patterns in the savannah monitor lizard. Nature 506, 367–370 (Data from: Dryad Digital Repository).
Schulp, A.S., Jagt, J.W.M., 2013. "Carlo", a new *Prognathodon*-like mosasaur from the type Maastrichtian. In: Polcyn, M.J., Jacobs, L.L. (Eds.), 4th Triennial International Mosasaur Meeting, May 20-25, Dallas Texas, p. 42.
Schulp, A.S., Vonhof, H.B., van der Lubbe, J.H.J.L., Janssen, R., van Baal, R.R., 2013. On diving and diet: resource partitioning in type-Maastrichtian mosasaurs. Netherlands Journal of Geosciences - Geologie en Mijnbouw 92, 165–170.
Schulp, A.S., Polcyn, M.J., Mateus, O., Jacobs, L.L., Morais, M.L., 2008. A new species of *Prognathodon* (Squamata, Mosasauridae) from the Maastrichtian of Angola, and the affinities of the mosasaur genus *Liodon*. In: Everhart, M. (Ed.), Proceedings of the Second Mosasaur Meeting, vol. 3. Fort Hays Studies Special Issue, pp. 1–12.
Schulp, A.S., Walenkamp, G.H.I.M., Hofman, P.A.M., Rothschild, B.M., Jagt, J.W.M., 2004. Rib fracture in *Prognathodon saturator* (Mosasauridae, Late Cretaceous). Netherlands Journal of Geosciences/Geologie en Mijnbouw 83, 251–254.
Schulp, A.S., Walenkamp, G.H.I.M., Hofman, P.A.M., Stuip, Y., Rothschild, B.M., 2006. Chronic bone infection in the jaw of *Mosasaurus hoffmanni* (Squamata). Oryctos 6, 41–52.
Silverman, S., 2006. Chapter 29: Diagnostic Imaging. In: Divers, S.J., Mader, D.R. (Eds.), Reptile Medicine and Surgery, second ed. Elsevier Health Sciences, Amsterdam, pp. 471–489.
Stacy, B.A., Pessie, A.P., 2007. Chapter 5: Host response to infectious agents and identification of pathogens in tissue section. In: Jacobsen, E.R. (Ed.), Infectious diseases and pathology of reptiles: color atlas and text. CRC Press, Boca Raton, pp. 257–298. Jacobsen, E.R. (Ed.).
Straight, W.H., Davis, G.L., Skinner, H.C.W., Haims, A., McClennan, B.L., Tanke, D.H., 2009. Bone lesions in hadrosaurs: Computed Tomographic Imaging as a guide for paleohistologic and stable-isotopic analysis. Journal of Vertebrate Paleontology 29, 315–325.
Tanke, D.H., Currie, P.C., 1998. Head-biting behaviour in theropod dinosaurs: Paleopathological evidence. Gaia 15, 167–184.
Williston, S.W., 1898. Mosasaurs. University Geological Survey of Kansas vol. 4 (5), 81–347 pls. 10-72.
Wolff, E.D.S., Salisbury, S.W., Horner, J.R., Varricchio, D.J., 2009. Common avian infection plagued the Tyrant Dinosaurs. PLoS One 4, 1–7.
Xing, L., Rothschild, B.M., Randolph-Quinney, P.S., Wang, Y., Parkinson, A.H., Ran, H., 2018. Possible bite-induced abscess and osteomyelitis in *Lufengosaurus* (Dinosauria: sauropodomorph) from the Lower Jurassic of the Yimen Basin, China. Scientific Reports 8, 5045.
Zimmerman, L.M., Vogel, L.A., Bowden, R.M., 2010. Commentary: Understanding the vertebrate immune system: insights from the reptilian perspective. Journal of Experimental Biology 213, 661–671.

Appendix ASupplementary data

Supplementary data to this article can be found online at https://doi.org/10.1016/j.cretres.2020.104425.